Journal of Siberian Federal University. Engineering & Technologies 2022 15(4): 459–471
~ ~ ~

DOI: 10.17516/1999-494X-0407

УДК 669.14.018.4:539.376

Study on Long-Term Tempering on the Microstructure of Creep Strength Enhanced Ferritic P92 Steel

Vinay Kumar Pal* **and L. P. Singh**
Sam Higginbottom University of Agriculture, Technology and Sciences
Allahabad, India

Received 02.04.2022, received in revised form 18.05.2022, accepted 24.06.2022

Abstract. Present paper deal with the studies of effect of long term heating on the microstructure and mechanical properties of creep strength enhanced Cr-Mo P92 steel. Such steels are used in supercritical power plant boilers where continuous operating temperature and pressure can be as high as 650 ^{0}C and 300 bar respectively. The P92 specimens were thermally exposed at temperature of 650 ^{0}C for duration of varying from 1000 to 3000 hours. Tensile fracture and impact toughness fracture surfaces were studied by using *scanning electron microscope.* The fracture surface of P92 impact toughness specimen exhibited both inter lath-decohesion and ductile dimple tearing. The various phases that formed in the tempered P92 steel were analyzed by X-ray diffraction. In XRD analysis of tempered P92 it was observed that amount of precipitates increased as compared to untempered condition. After tempering time of 1440 h, some new precipitates such as NbC, NbCrN were also observed.

Keywords: empering time, creep strength enhanced ferritic steel, grain, recipitates, $M_{23}C_6$, particles, microstructure.

Citation: Pal, V. K., Singh, L. P. Study on long-term tempering on the microstructure of creep strength enhanced ferritic P92 steel. J. Sib. Fed. Univ. Eng. & Technol., 2022, 15(4), 459–471. DOI: 10.17516/1999-494X-0407

* Corresponding author E-mail address: gaurishankar.vinaypal@gmail.com, vinaymd002@gmail.com

Исследование влияния длительного отпуска на микроструктуру ферритной стали P92 с повышенной прочностью на ползучесть

В. К. Пал, Л. П. Сингх
Университет сельского хозяйства, технологий и наук Сэма Хиггинботтома
Индия, Аллахабад

Аннотация. Настоящая работа посвящена исследованию влияния длительного нагрева на микроструктуру и механические свойства стали Cr-Mo P92 с повышенной прочностью на ползучесть. Такие стали используются в котлах сверхкритических электростанций, где постоянная рабочая температура и давление могут достигать 650 ºС и 300 бар соответственно. Образцы P92 подвергались термической обработке при температуре 650 ºС в течение от 1000 до 3000 часов. Поверхности разрушения при растяжении и ударной вязкости были изучены с помощью сканирующего электронного микроскопа. На поверхности разрушения образца ударной вязкости P92 наблюдались как межреберная декогезия, так и разрыв пластичных углублений. Различные фазы, образовавшиеся в закаленной стали P92, были проанализированы методом рентгеновской дифракции. При рентгеноструктурном анализе закаленного P92 было замечено, что количество осадков увеличилось по сравнению с нетвердым состоянием. После времени выдержки 1440 ч также наблюдались некоторые новые осадки, такие как NbC, NbCrN.

Ключевые слова: время отпуска, повышенная прочность стали на ползучесть, зерно, осадки, $M_{23}C_6$, частицы, микроструктура.

Цитирование: Пал, В. К. Исследование влияния длительного отпуска на микроструктуру ферритной стали P92 с повышенной прочностью на ползучесть / В. К. Пал, Л. П. Сингх // Журн. Сиб. федер. ун-та. Техника и технологии, 2022, 15(4). С. 459–471. DOI: 10.17516/1999-494X-0407

1. Introduction

Thermal power plants using CSEF steels having always a risk of damage due to creep deformation. For such type of application a routine checking of CSEF P92 steels is needed after a certain period of time to avoid catastrophic failure. The effect of long-term ageing on precipitate evolution behavior and room temperature tensile properties of P92 steel were also performed by many of researchers. Paul et al. [1] had studied the effect of long termageing on microstructure evolution of P92 steel in service temperature range of 500–600 °C. The lath structure was retained even after ageingup to 10000 h. A continuous coarsening was observed for $M_{23}C_6$ type carbide with exposure time and temperature while negligible coarsening was reported for V and Nb-rich carbide. A continuous increase in Cr/Fe ratio was also observed with increase in ageing time. Laves phase formation was reported after the ageing upto 5000 h that led to increase in DBTT. Homolova′ et al. [2] studied the thermal deformation history on microstructure evolution and stability of P92 steel in the temperature range of 580–650 °C. For low-temperature range (580–620 °C), Laves phase formed after the long duration while for the sample without deformation produced Laves phase after 1000 h annealing at 650 °C. For all temperature, Cr/Fe ratio in $M_{23}C_6$ increased with ageing time. Kafexihu et al. [3] performed ageing of P91 and X20CrMoV121 steel at 650 and 760 °C for varying ageing time (2 h, 4320 h, 8760 h and 1752 h). A Study was performed related to room temperature

tensile properties and hardness after long termageing. It was observed that tempering at 650 °C have arelatively small effect on mechanical properties as compared to tempering at 760 °C. Senior et al. [4] studied the effect of ageing on plastic behavior of 9Cr-1Mo steel. A continuous reduction in ductility was observed with increase in ageing time. The ductility failure was mainly led by inclusion and precipitate nucleated voids. The reduction in ductility after 1000 h was attributed to nucleation of voids on carbide particles. After 5000 h, Laves phase formation was observed that provided void nucleation sites and led to are duction in ductility. After Laves phase formation, void nucleation rate at carbides was decreased. Sathyanarayanan et al.[5] have studied the effect of ageing temperature and time on DBTT of P92 steel by using the reference temperature approach under dynamic loading condition (T_o^{dy}). At 650 °C, a drastic increase in T_o^{dy} was observed while at 600 °C, a moderate increase was observed. Ageing in the temperature range of 600–650 °C for 10000 h resulted in the formation of Laves phase that led to embrittling effect and ultimately increase in T_o^{dy}. Golañski and Kepa [6] performed the ageing of cast P92 steel and studied their effect on microstructure evolution and mechanical properties. The ageing was performed in the temperature range of 550–600 °C for varying ageing time (2000 h and 6000 h). Ageing up to 6000 h have found a negligible effect on the tensile properties, hardness and lath morphology of P92 steel. Ageing resulted in a drastic decrease in Charpy toughness value. The decrease in Charpy toughness value was attributed to the formation of Laves phase after long-term ageing of 6000 h.

The present research is primarily focused on effect of tempering on development of precipitates, size of precipitates and grain coarsening were studied. The study of long term heating at 650 ^{0}C on microstructure mechanical properties of P92 CSEF steels. The effect of long term tempering on fracture modes of P92 steel were studied.

2. Experimental details

The chemical composition of as-received material P92 steel as given in Table 1 was analyzed by using an optical emission spectrometer (Make: Metavision, model: 1008i). P92 ferritic steel pipe having 60.3 mm outer diameter and 11 mm thickness was used for the present investigation

The mechanical properties of the as-received material are depicted in Table 2.In the “as-received” condition, the P92 steel pipes were austenitized at 1040 °C for 10 min and air cooled, and then tempered at 760 °C for 2 h and finally air cooled. Before microstructure examination, the P92 samples were tempered at 650 °C with duration of tempering varying from 720 to 3000 hours. Tempering of specimens was performed in furnace under protective layer of Al_2O_3 and FeCr powder mixture.

The “as-received” condition, the P92 steel pipes were austenitized at 1040 °C for 10 min and air cooled, and then tempered at 760 °C for 2 h and finally air cooled. The mechanical properties of the as-received material are depicted in Table 2. Before microstructure examination, the P92 samples

Table 1. Chemical composition of the P92 steel

Element	Chemical composition, wt%												
	C	Mn	W	S	Si	Cr	Mo	V	N	Ni	Cu	Nb	Ti
Base metal	0.1457	0.5433	<0.01	0.0114	0.2748	8.4864	0.9481	0.1362	<0.02	0.3515	0.0589	<0.008	.0117

Table 2. Mechanical properties of P92 steel in as received state

P92 steel	Yield strength(MPa)	Tensile strength(MPa)	Elongation (%)	Hardness (HV)	Toughness(J)
	473	714	19	247	198

were tempered at 650 °C with duration of tempering varying from 720 to 3000 hours. Tempering of specimens was performed in furnace under protective layer of Al_2O_3 and FeCr powder mixture.

Tensile tests of P92 specimens at room temperature in as received condition were performed at normal strain rate of 1.66×10^{-5} /s with INSTRON 5982 vertical tensile testing machine. Specimens sectioned from tempered samples of P92 were subsequently tensile tested. Flat tensile test specimens having gauge length 25 mm were prepared as per ASTM E 8–04. To perform the Charpy impact test of tempered specimens, sub size specimens (55*10*7.5 mm^3) with 2 mm central V shaped notch were prepared. For each test condition, three tests were performed and the averages of three tests were noted.

In order to characterize the effect of tempering on microstructure evolution, grain size, secondary phase precipitates and their size, metallographic investigation were carried out by using optical microscope (OM) and scanning electron microscope (SEM) at different magnifications. Optical microscopy was performed on Dewinter LT-23. Band samples were primed by mechanical grinding, polishing up to 2000 grit size and etching with Villela solution (100ml of ethanol, 1 g of picric acid and 5 ml of hydrochloric acid). The samples prepared for optical microscopy were also used for SEM. QUANTA 200 Field scanning electron microscope was used to characterize the microstructure at different magnification of 5000X, 10000X and 50000X with accelerating voltage of 20 kV, 10-nA probe current for working distance of 8 mm. X-ray diffraction (XRD) of the samples was carried out by using the D-8 Bruker AXS diffractometer. XRD analysis was carried out by using by using Cu-target, with the working voltage and current of 40 kV and 30 mA respectively.

Hardness measurement was performed for P92 steel in as-delivered state as well as after tempering. The hardness of the samples was measured by using Vickers hardness tester (Omnitech-S. Auto) at the load of 500 gm and dwell time of 10 sec. The effect of tempering on fracture mechanism of tensile as well as impact tested specimen at room temperature, SEM analysis was carried out. Room temperature tensile and impact tests were performed for P92 steel in as–received state as well as after tempering. FE-SEM was used to characterize the effect of tempering on element percentage present at the fracture surface of tensile and impact tested specimens. SEM image at higher magnification, i.e.20000X were used to measure the size of void and ductility present at the fracture surface of room temperature tensile tested specimens.

3. Result and discussion

3.1. Optical micrograph

characteristic optical micrograph of P92 steel for the differentageing condition is depicted in Fig. 1(a-d). The effect of long-term ageing on the grain size of P92 steel is depicted in Fig. 1(e). In as-received condition, grain size was measured to be 41±10 μm. After the thermal ageing, optical micrograph does not show any significant change except the grain coarsening. The lath morphology of P92 steel is retained even after 3000 hrs of ageing. Heterogeneity is observed in grain size for the

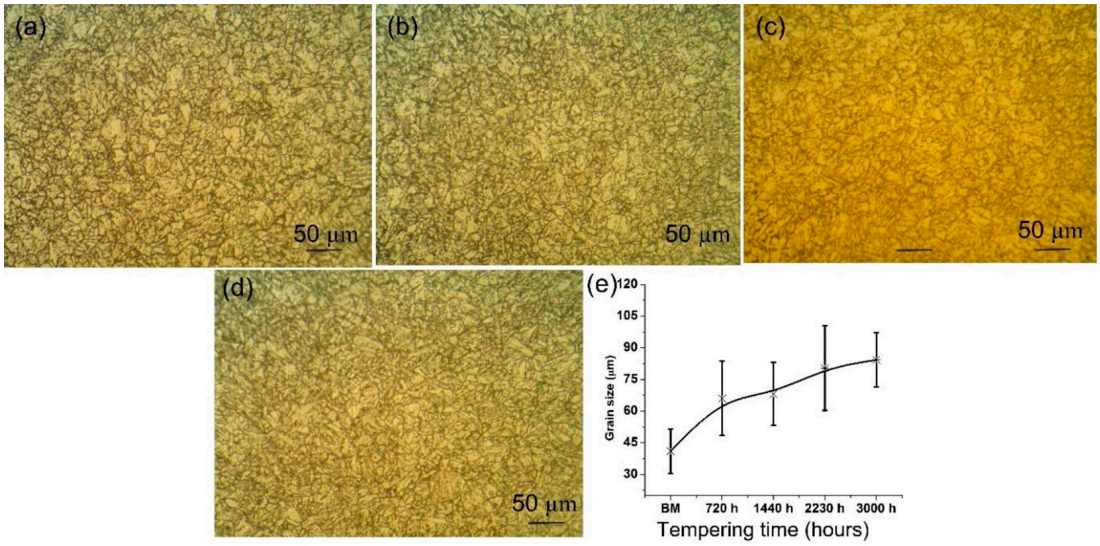

Fig. 1. Characteristic optical micrograph of P92 steel after ageing at 650 °C for ageing time of (a) 720 hrs, (b) 1440 hrs, (c) 2230 hrs, (d) 3000 hrs and (e) variation in grain size with ageing time.

differentageing condition. Initially, during ageing at 650 °C for 720 h, large amount of grain coarsening occurs and size of grain increases from 41 µm to 66 µm. A negligible change is observed with further increase in ageing time from 720 h to 1440 h (66µm to 68 µm). After tempering of 3000 h, the grain size is measured about 84 µm, which was an most double compared to as-received P92 steel.

3.2. SEM micrograph and particle size distribution

the Microstructure evolution and distribution and morphology of precipitates for the different ageing condition are shown in Fig. 2(a-h). The microstructure consists of equiaxed tempered laths with precipitates. In the initial stage of ageing, the evolution of new fine MX and coarse $M_{23}C_6$ precipitates occur. The morphology and distribution of precipitates inside the tempered laths are shown in higher magnification micrographs.

The coarse precipitates located along the PAGBs and lath boundaries show the different morphology like globular, lenticular and cylindrical. At higher magnification, fine precipitates inside the intra-lath region are observed having as pherical shape. With the increase in ageing time, number density and size of precipitates along the PAGBs are observed to be increased. For 720–1440 hrs ageing time, the precipitates decorated along the lath and PAGBs are observed to be needle, platelets and cylindrical shape. Some needle and platelets shape precipitates are also observed inside the intra-lath region. With the increase in ageing time from 1140 hrs to 2230 hrs, the number density of globular shape precipitates increased. For the geing time of 3000 hrs, very few needle and cylindrical shape precipitates are observed, as shown in Fig. 2(h). Lath morphology of tempered martensite is retained up to ageing time of 3000 hrs.

Variation in size and fraction area of precipitates is given in Fig. 3. For exposure temperature below than 650 °C and exposure time lower than 10^5 hrs, fine MX precipitates show the higher stability against coarsening [7,8]. Hence, it can be said that during ageing up to 3000 hrs, coarsening occurs only for $M_{23}C_6$ precipitates and size of MX precipitates remain stable. After ageing up to 720 hrs, size

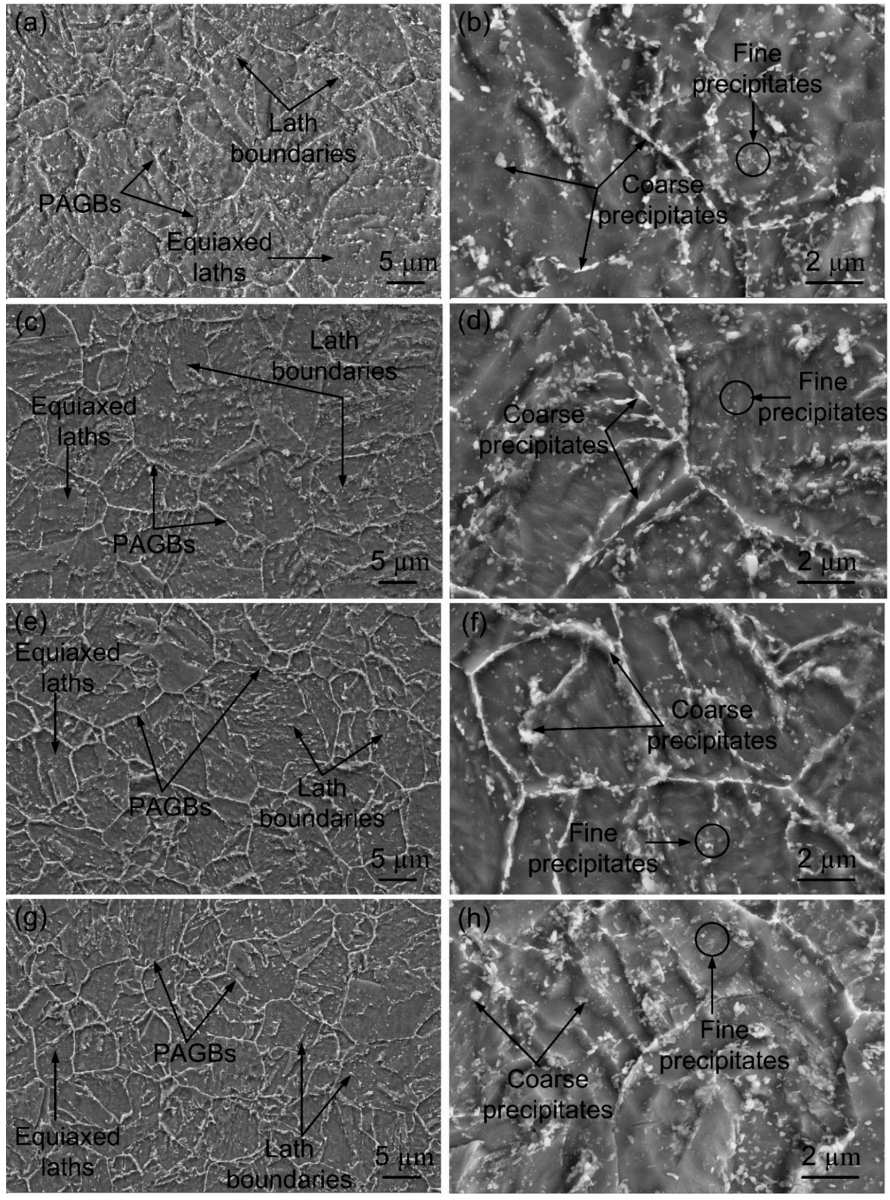

Fig. 2. Change in microstructure of P92 steel as a function of ageing time at 650 °C in low and high magnification (a) and (b) 720 hrs, (c) and (d) 1440 hrs, (e) and (f) 2230 hrs, (g) and (h) 3000 hrs.

of precipitates is observed to be varied from 17 to 288 nm. The size of $M_{23}C_6$ precipitates varies from 61–288 nm. The average size of $M_{23}C_6$ precipitates is measured 154±20 nm. The initial stage of ageing shows the evolution of new precipitates (size < 25 nm) and coarsening of existing precipitates. Particle size and their distribution are observed to be almost similar to the ageing time of 720 hrs and 1440 hrs. The size of $M_{23}C_6$ precipitates varies from 62 to 289 nm with the average precipitate size of 161±37 nm. With further increase in ageing time from 1440 hrs to 2230 hrs, average precipitate size did not show any change and it was measured to be 161±39 nm. The coarsening of precipitates are measured for the ageing time of 2230 hrs and size of $M_{23}C_6$ type precipitate varies from 87 to 311 nm. For the ageing time of 3000 hrs, a drastic increase is observed in precipitate size and average precipitate size

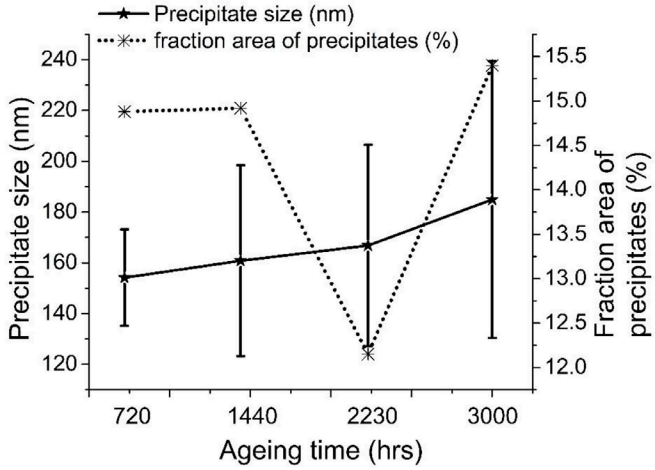

Fig. 3. Variation in size of precipitates size and fraction area of precipitates with ageing time.

is measured to be 185±54 nm. The size of $M_{23}C_6$ precipitates is observed to be varied from 97 to 421 nm. A great heterogeneity in size of precipitates is observed for ageing time of 3000 hrs, as shown in Fig. 3. In given ageing time range, size of MX precipitates was considered to be constant because of their higher thermal stability while in each ageing condition, precipitates having a size in the range of 17 to 45 nm were observed. Variation in fraction area of precipitates with ageing time is given in Fig. 3. After 720 hrs ageing, it was measured to be 14.88 %. In ageing time range of 720 to 1440 hrs, fraction area of precipitates remains constant. Increase in ageing time from 1440 to 3000 hrs, a drastic decrease is observed and it decreases from 14.92 % (1440 hrs) to 12.15 % (2230 hrs). The decrease in fraction area of precipitates indicates the coarsening of precipitates. Further increase in ageing time form 2230 hrs to 3000 hrs, it increases from 12.15 % to 15.38 %. Increase in fraction area of precipitates indicates the new secondary phase formation. The number density of fine MX precipitates is also observed to be increased for the ageing time of 3000 hrs, as shown in Fig. 3.28(h). Hence, for 3000 hrs ageing, both coarsening and evolution of precipitates were observed.

The coarsening of $M_{23}C_6$ precipitates during the long-term ageing occur by the Ostwald ripening mechanism [6]. The coarsening of $M_{23}C_6$ precipitates leads to decrease in the number density of precipitates while volume fraction remains constant. The decrease in the number density of $M_{23}C_6$ precipitates results in a reduction in pinning effect for coarsening of laths and PAGBs that affects the polygonization of the matrix. Apart from the coagulation and precipitation of $M_{23}C_6$ carbides during ageing, the recovery process and matrix polygonization were observed to be running.

The EDS spectra of $M_{23}C_6$ precipitates for the ageing time of 720 hrs and 3000 hrs are shown in Fig. 4 (a) and (b), respectively. $M_{23}C_6$ precipitates are observed to be enriched with Cr, Fe, and Mo, as shown in Fig. 4. With the increase in ageing time percentage of Cr in $M_{23}C_6$ increased while Fe and Mo percentage decreased. So it can be inferred that increase in ageing time leads to change in chemical composition of $M_{23}C_6$ carbides and get enriched in Cr, i.e. $M_{23}C_6$ mainly replaced by $Cr_{23}C_6$. Compositional variation for $M_{23}C_6$ carbide is shown in Fig. 4(c). A small amount of V and Nb are also observed in $M_{23}C_6$ carbides at the initial stage of ageing while after 3000 hrs of ageing only V was observed. Cr/Fe ration was observed to be increased continuously with ageing time while Mo/Fe

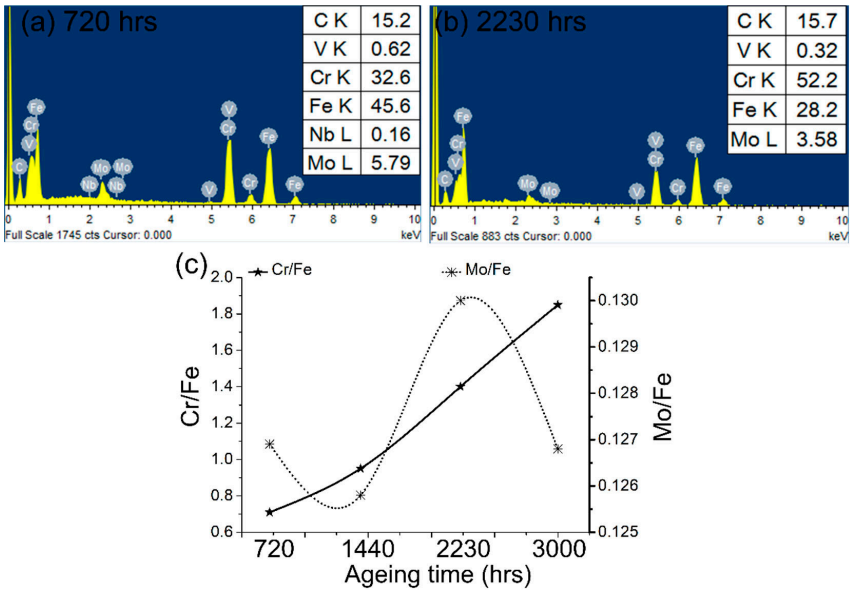

Fig. 4. EDS spectra of $M_{23}C_6$ precipitates after ageing at 650 °C for ageing time of (a) 720 hrs, (b) 3000 hrs and (c) variation in composition of $M_{23}C_6$ carbide as function of ageing time.

ratio remained almost constant. A continuous increase in Cr/Fe ratio with ageing time is attributed to thermal driven diffusion of Cr into carbides and leads to the evolution of Cr-rich meta-stable $M_{23}C_6$ phase. The similar results have also been reported by Paul et al. [1]. Cr and Mo-rich Laves phase $(Cr, Fe)_2$ (W, Mo) was not observed in EDS spectra. In P92 steel, Laves phase formation was generally observed after the ageing up to 5000 hrs. For the confirmation of phases, XRD analysis was also performed [1,4].

3.3. XRD analysis

Diffractograms of P92 steel in different ageing conditions are presented in Fig. 5(a-d). After ageing at 650 °C for 720 h, the new low intensity peak at 37.76° is observed that confirms the $Cr_{23}C_6$, VC, VN, NbN, and Cr_2N phase. Peaks of phases like $Mn_{23}C_6$, Mn_7C_3, Fe_7C_3, and Fe_3C are not observed after the ageing. It might be assumed that the unseen phases after the ageing are transformed to more stable $M_{23}C_6$ phase. The similar phases were also observed for ageing time of 1440 hrs, as shown in Fig. 5(b). From Fig. 5(c), after 2230 h of ageing, Nb-rich NbC phase was observed. Paul et al. had reported that after long-term ageing, fine MX precipitates were observed to be Nb-rich because of higher thermal stability of NbC as compared to VC. No change in phase evolution was observed with further increase in ageing time from 2230 hrs to 3000 hrs, as shown in Fig. 5(d). No peaks of Laves phase were observed up to the ageing time of 3000 hrs. The EDS spectra of precipitates also confirmed the absence of Laves phase.

3.4. Room temperature mechanical properties

Fig. 6 shows the variation in mechanical properties of P92 steel after ageing at 650 °C in the time range of 720–3000 hrs. Degradation in ultimate tensile strength (UTS) and yield strength (YS) with an

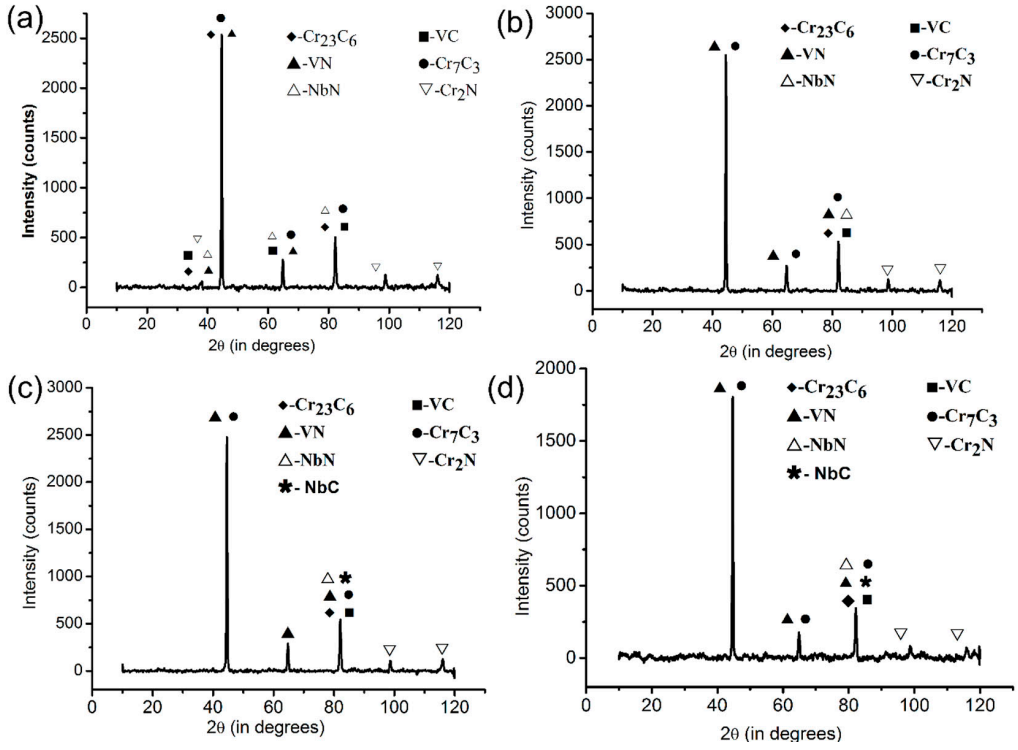

Fig. 5. X-ray diffraction pattern for P92 steel for different ageing time (b) 720 hrs, (c) 1440 hrs, (d) 2230 hrs and (d) 3000 hrs.

increase in ageing time are clearly seen from Fig. 6(a). The YS drops by 43 MPa and UTS by 48 MPa after ageing up to 3000 hrs. The reduction in YS and UTS are attributed to softening effect that occurs due to grain coarsening and thermal straining of precipitates. Ageing time up to 1440 hrs, YS and UTS have observed no significant change but after that, a sudden drop occurs in UTS value. The thermal straining of precipitates is also observed to be significant after the ageing of 1440 hrs. Figure 6(b) shows the effect of ageing time on% reduction in area and% elongation and it was observed that% reduction in area and% elongation increased continuously with increase in ageing time. Maximum percentage elongation and percentage reduction in the area are measured 28.5±1.5 and 75±2 %, respectively for the ageing time of 3000 hrs.

Variation in hardness with ageing time is given in Fig. 6(a). At the initial stage of ageing (720 hrs), softening effect results in a sudden drop of micro hardness and it was measured about 221±5 HV. The reduction in microhardness remains continues up to ageing time of 1440 hrs. The micro hardness depends on too many factors like precipitation hardening, solid solution hardening, sub-grain hardening and lath widening. For an ageing time up to 1440 hrs, grain coarsening and precipitate coarsening effect dominates over the others. Ageing after the 1440 hrs leads to a sudden increase in microhardness value. The increase in micro hardness indicates that the softening behaviour of P92 steel due to recovery has been hindered by other changes in fraction area of precipitates and formation of secondary phases. After 1440 hrs, a sudden drop in fraction area of precipitates was observed that led to higher carbon and nitrogen in solution matrix. Higher C and N in solution matrix leads to solid

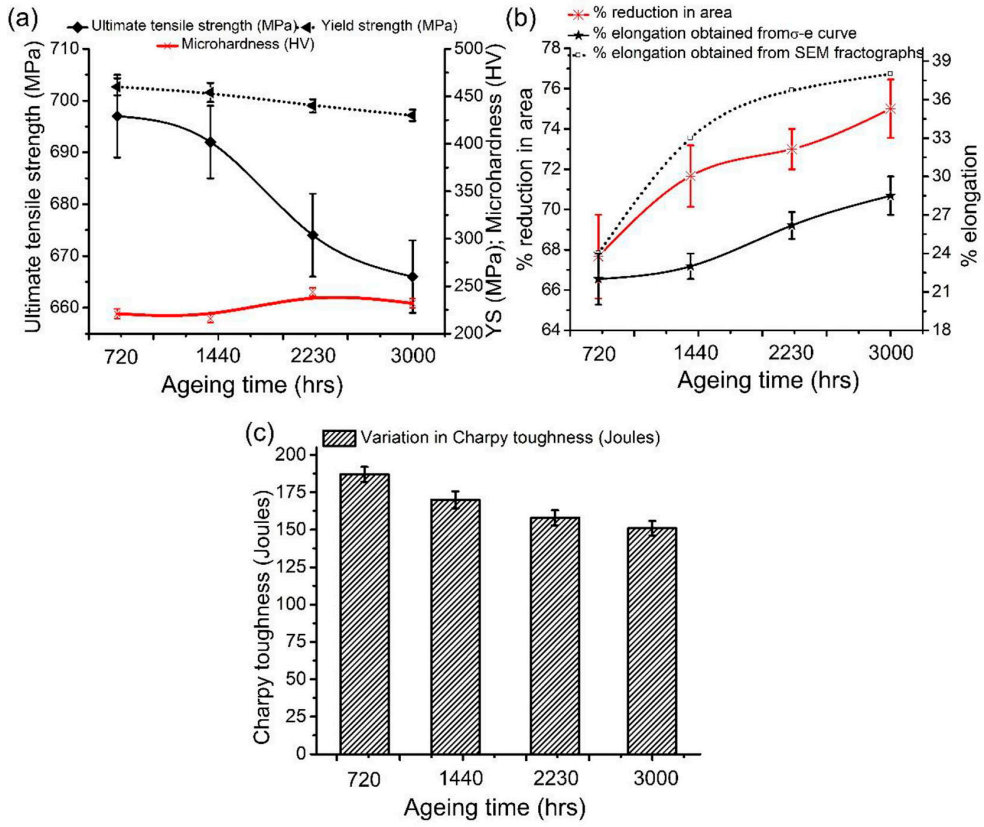

Fig. 6. Variation in mechanical properties with ageing time (a) variation in UTS, YS and hardness, (b) variation in% elongation and% reduction in area and (c) variation in Charpy toughness.

solution hardening that results in higher microhardness for the ageing of 2230 hrs. After the 2230 hrs, a further decrease in microhardness was observed. The microhardness value indicates the saturation. The decrease in microhardness attributed to increasein fraction area of precipitates after the 2230 hrs. That leads to a reduction in solid solution hardening. The higher thermal straining of precipitates after 2230 hrs might be the cause of reduction in microhardness value. After 3000 hrs of ageing, the hardness of P92 steel was reduced by 15 HV compared to the as-received material.

Reduction in strength and hardness are accompanied by considerable lowering in Charpy toughness value from 198±8 Joules in 'as-received' condition, to value of 151±5 Joules after the ageing of 3000 hrs. Variation in room temperature Charpy toughness of P92 steel with ageing time is shown in Fig. 6(c). Charpy toughness was observed to be decreased continuously with increase in ageing time. The decrement in Charpy toughness value is mainly related to cracking of secondary phase particles during thermal straining and decohesion at precipitates and matrix interface. After ageing of 3000 hrs, undoubtedly 24 % reduction in Charpy toughness value is attributed to coagulation and higher thermal straining of $M_{23}C_6$ precipitates on PAGBs.

3.5. FESEM analysis of fracture surface after interrupted tensile test

Effect of ageing time on fracture surface morphology of room temperature tensile tested specimens is shown in Fig. 7(a-d). The higher magnification fractographs (top right in the figure) shows

the distribution of micro voids and cleavage facets at the fracture surface and used for determining the ductility and size of micro-voids present at the fracture surface. The detailed view of fracture surfaces indicates the mixed mode of fracture, consisting of coalescence of micro-voids and trans-granular cleavage facets. At the initial stage of ageing (720 hrs), fracture surface reveals the presence of cleavage facets, ductile dimples, cleavage facets and microvoids. The number density of micro voids is observed to be less. The size of voids is measured 369 nm which is much higher than void size present at the fracture surface of the tensile tested as-received material, as shown in Fig. 7(e). With the increase in ageing time, trans-granular cleavage facets and are observed to be decreased. The number density of fine dimples and microvoids increased at the fracture surface and size of voids were measured to be 298 nm, as shown in Fig. 7(e).The detailed view of the racture surface of tensile specimens, after the ageing time of 2230 hrs and 3000 hrs are presented in Fig. 7(c) and (d), respectively. With the increase in ageing time from 1440 hrs to 3000 hrs fracture mode remains same. However, number density and size of microvoids are increased. Presence of cleavage facets at the fracture surface is decreased with increase in ageing time. Ageing for 2230 hrs at 650 °C resulted in an increase in the size of voids compared to base metal and sample aged at 720 and 1440 hrs. The voids are generally nucleated at the coarse carbide particles. After 2230 hrs, coarsening of carbide precipitates has been already reported in Fig. 7.

Senior et al. [4] had suggested that phosphorous segregation at the carbide matrix interface might be the possible cause of the reduction in strength and increase in the size of voids. With further increase in ageing time from 2230 hrs to 3000 hrs, size of micro voids increased, as shown in Fig. 7(e). The increase in the size of micro voids is further attributed to coarsening of carbide precipitates that provide the void nucleation sites. The fracture surface of tensile specimens at higher magnification is useful to predict the ductility behavior of P92 steel in different ageing conditions. Ductility obtained from SEM of the fracture surface is shown in Fig. 7(d). The ductility obtained with SEM micrograph shows a close agreement with the value obtained from stress-strain curve. The maximum deviation of 35 % was obtained for the ageing time of 3000 hrs. In contrast, there was no any correlation was observed between the ductility obtained

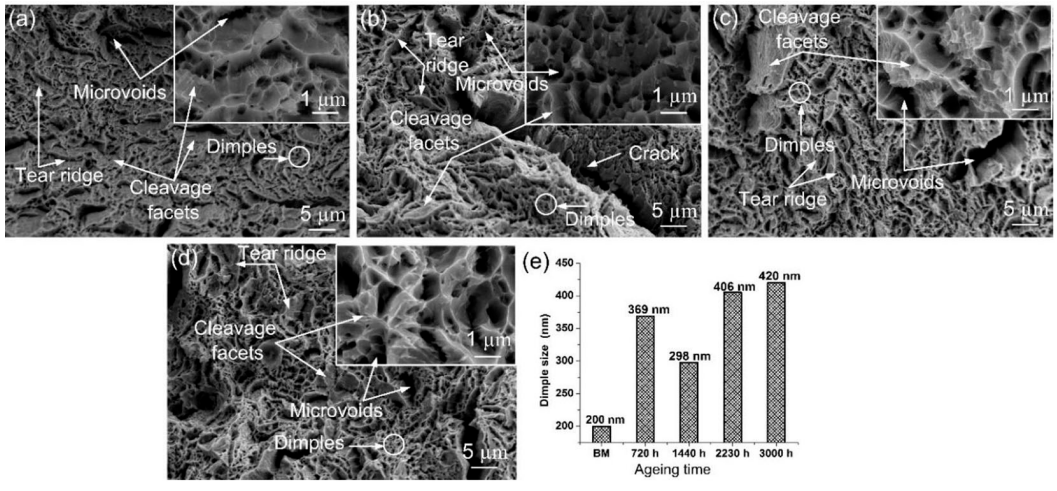

Fig. 7. Fractographs of room-temperature tensile tested specimen for different ageing time (a) 720 hrs, (b) 1440 hrs, (c) 2230 hrs, (d) 3000 hrs and (e) effect of ageing on dimples size present at fracture surface.

from the stress-strain curve and ductility calculated from the micro voids and ductile dimples present at the fracture surface. The continuous nucleation of voids at the carbide precipitates might be the main cause of the reduction in strength of P92 steel with ageing time.

4. Conclusion

The present research work investigates the effect of the long-term ageing on the microstructure of creep strength of P92 steel. The following conclusions can be drawn:

1. Long term tempering of P92 at 650 °C for different tempering time was marked with reduction in yield strength and ultimate strength. The yield strength reduced by 43 MPa and tensile strength by 48 MPa after tempering up to 3000 h. Tempering of P92 led to heterogeneity in the distribution and size of carbide precipitates. The average size of carbide particles increased after tempering of 3000 h from 137 nm (in as-received state) to 185 nm.

2. With increase in tempering time, chemical composition of $M_{23}C_6$ (M: Cr, Mn, Fe, Mo) particles changed and became enriched in Cr as $M_{23}C_6$ mostly replaced by $Cr_{23}C_6$.

3. Similar to as-received condition, $Cr_{23}C_6$, VC, VN, NbC, NbN, $Mn_{23}C_6$, Cr_7C_3, and Fe_7W_6 were the main precipitates that were observed in P92 steel after long term tempering at 650 °C. No peaks of laves phase (Fe_2W, Fe_2Mo, Cr_2W, and Cr_2Mo) were observed up to 2230 h tempering. Z-phase (NbCrN) formation occurred after tempering up to 1440 h.

4. Increase in duration of tempering time led to decrease in impact toughness possibly due to cracking of secondary phase particles during straining and decohesion at precipitates and matrix interface. After tempering of 3000 h, the impact toughness of P92 samples reduced by 25 % compared to as received condition.

5. After 3000 h of tempering at 650 °C, the hardness of P92 reduced by 15 HV. Compared to yield strength and tensile strength, the tempering time has less severe effect on hardness.

References

[1] Thomas Paul V., Saroja S., Vijayalakshmi M. Microstructural stability of modified 9Cr-1Mo steel during long term exposures at elevated temperatures, *J. Nucl. Mater*, 378 (2008) 273–281. https://doi.org/10.1016/j.jnucmat.2008.06.033.

[2] Homolova V., Janovec J., Zahumensky P., Vyrostkova A. Influence of thermal-deformation history on evolution of secondary phases in P91 steel, *Mater. Sci, Eng. A.* 349 (2003) 306–312.

[3] Kafexhiu F., Vodopivec F., Turna J. V. Effect of tempering on the room-temperature mechanical properties of X20CrMoV121 and P91 steels, *Mater. Tehnol,* 46 (2012) 459–464.

[4] Senior B.A., Eyres B. L., Avenue K., House C. The effect of ageing on the ductility of 9Cr-l Mo steel, *Acta Mater,* 36 (1988) 1855–1862.

[5] Sathyanarayanan S., Basu J., Moitra A., Sasikala G. Effect of thermal aging on ductile-brittle transition temperature of modified 9Cr-1Mo steel evaluated with reference temperature approach under dynamic loading condition, *Metall. Mater. Trans. A,* 44 (2013) 2141–2155. https://doi.org/10.1007/s11661–012–1510–0.

[6] Golañski G., Kepa J. The effect of ageing temperatures on microstructure and mechanical properties of GX12CrMoVNbN 9–1 (GP91) cast steel, *Arch. Metall. Mater,* 57 (2012) 575–582. https://doi.org/10.2478/v10172–012–0061–0.

[7] Hald J. Microstructure and long-term creep properties of 9–12 % Cr steels, *Int. J. Press. Vessel. Pip*, 85 (2008) 30–37. https://doi.org/10.1016/j.ijpvp.2007.06.010.

[8] Sawada K., Kubo K., Abe F. Contribution of coarsening of MX carbonitrides to creep strength degradation in high chromium ferritic steel, *Mater. Sci. Technol,* 19 (2003) 732–738. https://doi.org/10.1179/026708303225010687.